Search for manifestations of space weathering among C- and S-type asteroid families

Oleksandr F. KHROMIUK
E-mail: *cfif200216@gmail.com*
ORCID: *https://orcid.org/0009-0009-6569-107X*

Ivan H. SLYUSAREV
E-mail: i.slyusarev@karazin.ua
ORCID: https://orcid.org/0000-0003-4919-8225

V.N. Karazin Kharkiv National University, Ukraine

Received April 26, 2026, in the final form June 9, 2026
https://doi.org/10.3842/kau.2026.phys.01

Abstract. We investigate the effects of space weathering in 24 asteroid families of different taxonomic classes (11 S-type and 13 C-type families) and ages using photometric data from the SDSS, Gaia DR3, and SkyMapper surveys. The age of each family was determined using the V-shape approximation in the semi-major axis – absolute magnitude space. In addition, we analyzed the spectral properties of family members and investigated the dependence of the a^* parameter, a proxy for spectral slope, on family age. Significant correlations between a^* and the logarithm of age were found for both S-type and C-type families. The results reveal distinct evolutionary trends in spectral slope: a^* decreases with age in C-type families, whereas it increases in S-type families. These findings provide new constraints on space-weathering processes and their effects on the surface properties of asteroids.

Keywords: space weathering; V-shape; color index; taxonomy; asteroid families; SDSS; Gaia; SkyMapper.

1 Introduction

Space weathering encompasses a suite of physicochemical processes that alter the surface properties of airless bodies as a result of prolonged exposure to the space environment. The principal agents driving these modifications are micrometeorite bombardment and irradiation by the solar wind and cosmic rays. Acting on cosmogonical timescales, these processes induce significant changes in the spectral, mineralogical, chemical, and morphological characteristics of the surfaces of asteroids, planetary satellites, and other small airless bodies throughout the Solar System. The Moon is the most extensively studied body for investigating space-weathering processes [7], which have been examined through both laboratory analyses of Apollo-returned samples and theoretical modeling. Although asteroids are subjected to broadly similar space-weathering agents, systematic investigations of these processes have become possible only within the last decade owing to advances in large-scale photometric surveys [8, 9] and the return of the first asteroid samples to Earth. Despite these developments, significant discrepancies remain between weathering timescales inferred from lunar regolith studies, laboratory experiments on meteorites, and telescopic observations of asteroids. Asteroid families represent an important tool for studying the evolution of space-weathering effects [2]. As fragments produced by the disruption of a common parent body, family members are expected to possess similar initial compositions and ages, providing an opportunity to investigate the cumulative effects of space weathering while reducing the influence of compositional variability [1]. Accordingly, this study examines the manifestations of space weathering in asteroid families that cover a wide range of taxonomic classes and formation ages.

2 Data and methodology

The SDSS MOC-4 catalog has long been the primary source of photometric data for asteroids. However, new surveys have emerged, including the SkyMapper survey and Gaia DR3. In addition, WISE satellite provides a catalog of more than 150,000 asteroids albedo and diameters [4]. These developments have provided comprehensive, high-quality datasets for studying asteroid physical properties, enabling systematic investigations of space-weathering effects and their variation with asteroid composition and age. This work proposes analyzing space weathering in asteroid families using albedo and the parameter a^* [3].

2.1 Color indicies and parameter a^*

Twenty-four asteroid families were selected for analysis: 11 S-type (Agnia, Barcelona, Eunomia, Gefion, Iannini, Karin, Koronis, Maria, Massalia, Merxia, Rafita) and 13 C-type (Adeona, Astrid, Dora, Erigone, Euphrosyne, Hoffmeister, Hygiea, Misa, Naema, Nemesis, Themis, Ursula, Veritas). The list of members for each family was taken from the Nesvorný catalog [6].

For all members of the families, a cross-search was performed in four photometric catalogs, and stellar magnitudes in the corresponding filters and their errors were obtained. Based on these data, the main color indices (g–r, r–i, etc.) and their errors were calculated. Objects with abnormal color values or relative errors greater than 0.50 were rejected from the sample.

The next step was to calculate the color index a^*, which was determined by formula [3]:

$$a^* = 0.89(g - r) + 0.45(r - i) - 0.57.$$

The next step involved conducting a cross-search for geometric albedo values for all 24 families using data from the WISE mission [4]. To refine the criteria for filtering out "contaminants" (asteroids of other taxonomic classes), the two-dimensional distribution of objects in the "albedo – a^*" parameter space was analyzed. The criterion used for exclusion was the detection of objects outside the main cluster (core) of a specific dynamic family. Visualization and statistical analysis of these relationships allowed for a clear distinction between members of the family's primary taxonomic type and nonfamily asteroids. In particular, for the S-complex asteroid families, both compact isolated groups of objects with low albedo ($p_v < 0.1$) and negative values of the a^* values, consistent with possible to contamination of the family by carbonaceous asteroids, and isolated outliers with unusually high color indices ($a^* > 0.6$), that deviate significantly from the main cluster (Figure 1).

All objects that fell into such isolated additional clusters or exhibited extreme outliers on the "albedo – a^*" plane were excluded from further analysis. This reduced the contamination from background main-belt objects and from members of nearby dynamical groups that were incorrectly assigned to the studied families due to limitations in automatic dynamical classification or overlaps in orbital element space.

2.2 Building a V-shape for asteroid families

For each of the 24 selected asteroid families from Nesvorný's catalog [6], we constructed graphs showing the dependence of absolute magnitude H on the proper semi-major axis a. Each point on the graph corresponded to a separate object in the family.

The resulting distributions were then approximated using the following formula [1]:

$$H = 5 \log_{10} \left(\frac{|a - a_c|}{C} \right)$$

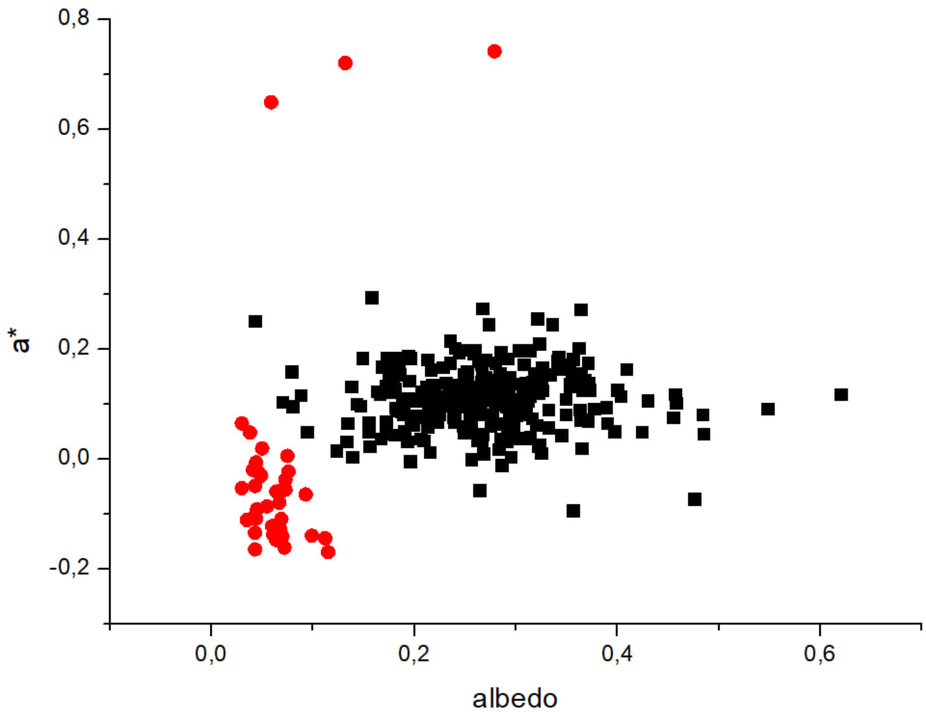

Figure 1. Distribution of asteroids in the Gefion family on the "albedo – a^*" plane. The main taxonomic core of the family is highlighted by black squares, while red circles indicate extraneous "impurities" (an additional cluster of C-type objects and excess anomalous points) that have been filtered out.

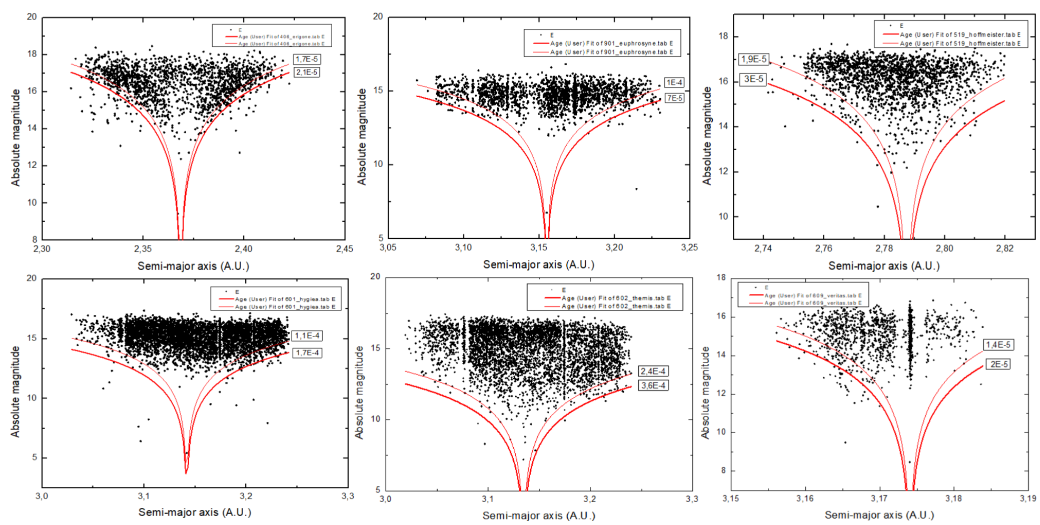

Figure 2. Constructed V-shapes and their approximations for C-type families.

where H is absolute magnitude, a is proper semi-major axis, a_c is center of the V-shape, C is width parameter. Parameter C is critical for determining the age of the family, as it reflects the rate of dispersion of fragments after the initial collision due to the Yarkovsky effect [11].

The reason for the emergence of such structures is the non-gravitational Yarkovsky effect, which leads to a change in the semi-major axis of an asteroid depending on its size and orientation of the axis of rotation. Thus, for each family, corresponding V-shapes were constructed with selected C values, which were used in further age calculations.

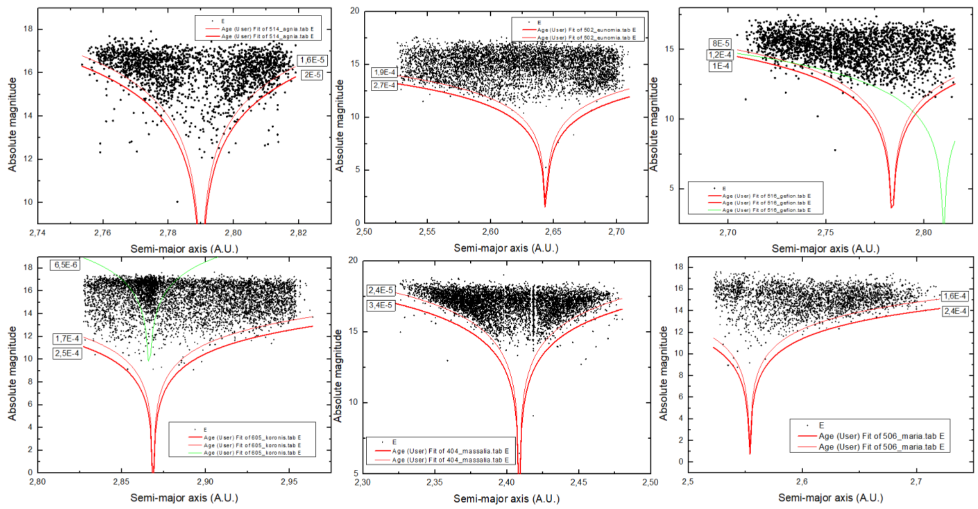

Figure 3. Constructed V-shapes for S-type families.

2.3 Age estimation

After constructing the V-shape for each of the 24 asteroid families, with the parameter C defined for each of them, the next step was to calculate their age. The basic idea is that, with increasing age, family members progressively spread along the major axis away from the family center; thus, the width of the V-shape provides a direct proxy for the family age. For a quantitative estimate, we adopt a semi-empirical formulation described by [6]:

$$t_{\rm age} \simeq 1\,{\rm g.y.} \times \left(\frac{C_0}{10^{-4}\,{\rm AU}}\right) \times \left(\frac{a_c}{2.5\,{\rm AU}}\right)^2 \times \left(\frac{\rho}{2.5\,{\rm g\ cm^{-3}}}\right) \times \left(\frac{0.2}{p_V}\right)^{\frac{1}{2}}$$

where $t_{\rm age}$ is age of the family (in billion years), C_0 is width of the V-shape, determined at the previous stage, a_c is central proper semi-major axis of the V-shape (the proper semi-major axis of the parent body in the formula for constructing the V-shape), ρ is average density of the family objects (in g/cm^3), p_V is mean geometric albedo.

The parameter C was selected individually for each family by visual adjustment of the V-shape, as the observed asteroid distributions in eigenspace deviate substantially from idealized theoretical models. In particular, real families often exhibit pronounced asymmetry between the two wings, as well as internal gaps and artificial boundaries caused by the dynamical effects of mean-motion and secular resonances. Under these conditions, formal mathematical criteria are overly sensitive to local density inhomogeneities and to the presence of background interlopers near the family boundaries, which can introduce significant systematic errors in the automatic determination of V-shape slopes. To mitigate these effects, we performed an individual selection procedure with a controlled shift of the family center a_c within the range 0.002–0.01 au, allowing us to account for dynamical distortions and to isolate the influence of resonance regions. The geometric albedo p_V was derived separately for each family using WISE data [4].

The average densities (ρ) were taken from Carry [8]: for S-types – 2.70 ± 0.69 g/cm^3, for C-types – 1.41 ± 0.69 g/cm^3.

Using the formula, we obtained approximate age estimates for each family – from several million to over a billion years. It should be noted that the error in age estimation is largely due to uncertainty in albedo and real differences in the density of individual objects in the family, as well as possible errors in our selection of the V-shape width.

3 Results and discussion

3.1 Dependence of a^* on age in S-types families

Using the previously calculated data, we analyzed the change in parameter a^* with respect to the age of S-type families and observed an increase in this parameter over time. This is consistent with the lunar case of space weathering, where the spectral slope increases with time. Within the 11 S-type families we selected, a positive correlation between age and the average value of parameter a^* can be clearly traced. A graph of a^* (for all four photometric catalogs) versus the age of families was constructed (Figure 4). The dependence is linear in logarithmic scale, which corresponds to theoretical expectations: the weathering process is more intense in the early stages (up to 700 Myr), after which the weathering rate slows down. This may explain the color saturation in older families.

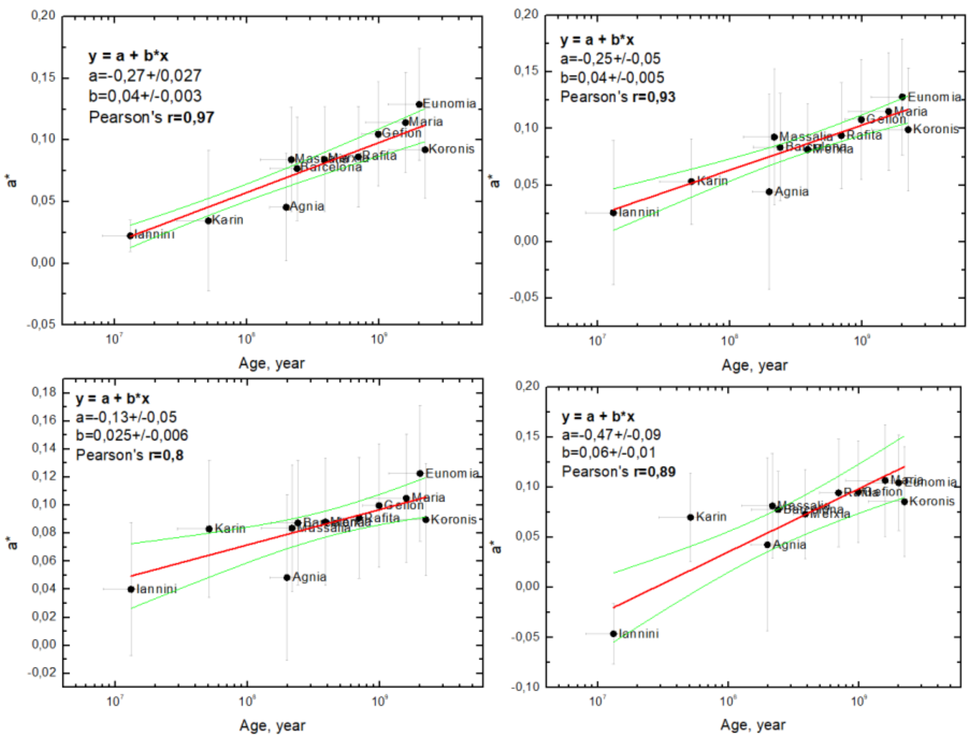

Figure 4. Dependence of the color index a^* on age for S-type families according to four photometric catalogs (top left – SDSS MOC4, right – SDSS [8], bottom left – Gaia, right – SkyMapper [9]).

3.2 Dependence of a^* on age in C-types families

For C-type families, the spectrum is less sensitive to space weathering than S-type families due to their dark, carbon-rich surface, which limits spectral changes in the visible range.

Among the 13 selected C-complex families, a weak but systematic decrease in the a^* spectral slope parameter with increasing age is observed, suggesting progressive "bluing" of the surface. Although the dependence is weaker and less stable than in the S-type, the general trend is confirmed by the a^* graph of the age of families (Figure 5).

This is commonly attributed to a more subdued or fundamentally different space-weathering regime acting on carbonaceous surfaces, or alternatively to compositional and regolith-structural effects that modulate optical maturation. In contrast to the logarithmic spectral reddening and eventual saturation observed for S-type asteroids, the C-complex appears to exhibit a more

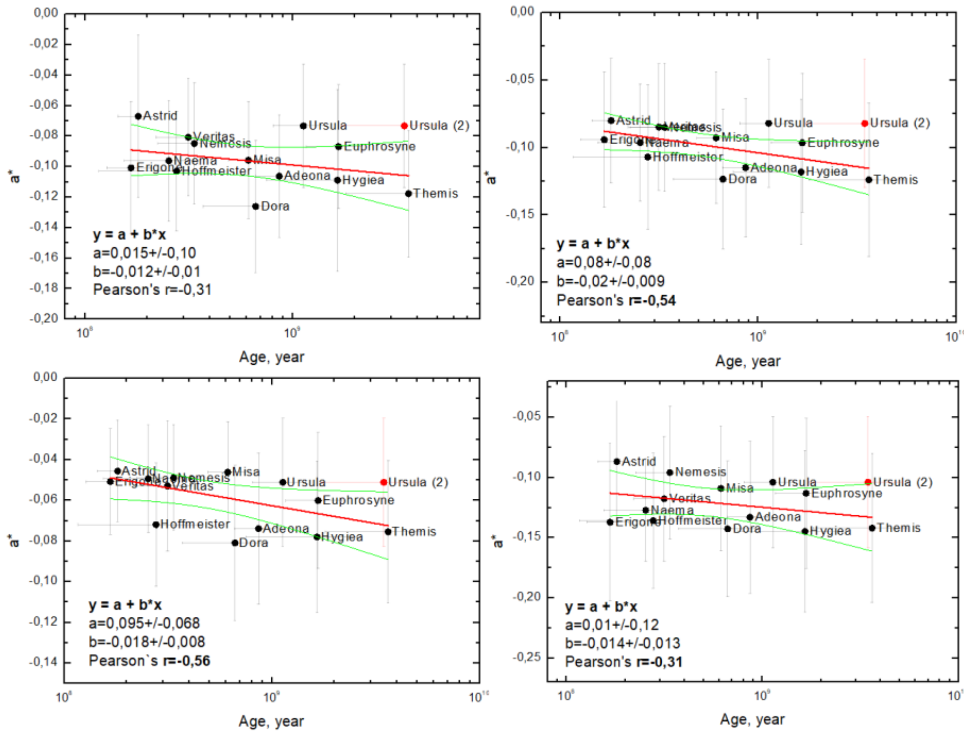

Figure 5. Dependence of the color index a^* on age for C-type families (top left – SDSS MOC4, right – SDSS (Sergeev), bottom left – GAIA [8], right – SkyMapper [9]).

gradual and less monotonic evolution in color indices. For C-type families, the variation in a^* with age is weaker and more dispersed, consistent either with slower weathering rates, more efficient optical resetting via collisional gardening, or intrinsically lower sensitivity of carbon-rich material to space-weathering products at visible wavelengths.

It should be noted that variations between individual families still remain and may be related to different proportions of secondary events, compositional features, or the accuracy of photometric data. However, even under such conditions, a general trend can be observed, which can be interpreted as an indicator of long-term surface "aging" under the influence of space weathering.

4 Conclusions

This article analyzes the manifestations of space weathering on the surface of S- and C-type families using four photometric catalogs (SDSS MOC4, Gaia DR3, SkyMapper, SDSS reprocessed by Sergeev) [8,9] and dynamic characteristics from the Nesvorný catalog [6]. The key parameters were the a^* index as an indicator of spectral evolution and the V-shape for estimating the age of the families.

The age of the families was calculated using the V-shape method with Nesvorný's formula [6], the results were compared with previous studies [6,11], and they are in good agreement.

For S-families, there is a clear increase in a^* with age, which is consistent with the model of space weathering and the accumulation of nano-phase iron ($npFe^0$). The graphs show an increase in the a^* parameter (slope of the spectrum) over time.

For C-families, a^* decreases with age, indicating a different nature of weathering processes on dark carbon-rich surfaces. Low albedo and spectral "flatness" complicate photometric analysis. The results highlight the differences in weathering mechanisms between S and C-types and the need for further spectroscopic and laboratory studies.

These results are consistent with the conclusions of David Nesvorný et al. [5], while extending them through a significantly enlarged sample of asteroid families and the use of four independent photometric catalogues.

References

[1] Gradie J.C., Chapman C.R., Williams J.G., Families of minor planets, in Asteroids, University of Arizona Press, Tucson, 1979, 359–390.

[2] Hapke B., Space weathering from Mercury to the asteroid belt, *J. Geophys. Res. Planets* **106** (2001), 10039–10073.

[3] Ivezić Ž. et al., Solar system objects observed in the Sloan Digital Sky Survey commissioning data, *Astron. J.* **122** (2001), 2749–2773.

[4] Masiero J.R. et al., Main belt asteroids with WISE/NEOWISE. I. Preliminary albedos and diameters, *Astrophys. J.* **741** (2011), 68, 20 pages.

[5] Nesvorný D. et al., Evidence for asteroid space weathering from the Sloan Digital Sky Survey, *Icarus* **173** (2005), 132–152.

[6] Nesvorný D., Brož M., Carruba V., Identification and dynamical properties of asteroid families, in Asteroids IV, University of Arizona Press, Tucson, 2015, 297–321, arXiv:1502.01628.

[7] Pieters C.M. et al., Space weathering on airless bodies: Resolving a mystery with lunar samples, *Meteorit. Planet. Sci.* **35** (2000), 1101–1107.

[8] Sergeyev S., Carry B., A million asteroid observations in the Sloan Digital Sky Survey, *Astron. Astrophys.* **652** (2021), A59.

[9] Sergeyev S. et al., Multifilter photometry of Solar System objects from the SkyMapper Southern Survey, *Astron. Astrophys.* **658** (2022), A109.

[10] Spoto F., Milani A., Knežević Z., Asteroid family ages, *Icarus* **257** (2015), 275–289, arXiv:1504.05461.

[11] Tholen D.J., Asteroid taxonomy from cluster analysis of photometry, Ph.D. Thesis, University of Arizona, 1984.

Дослідження проявів космічного вивітрювання серед сімейств астероїдів C- та S-типів

Олександр Ф. ХРОМЮК
E-mail: *cfif200216@gmail.com*
ORCID: *https://orcid.org/0009-0009-6569-107X*

Іван Г. СЛЮСАРЕВ
E-mail: *i.slyusarev@karazin.ua*
ORCID: *https://orcid.org/0000-0003-4919-8225*

Харківський національний університет імені В.Н. Каразіна, Україна

Отримано 26 квітня 2026, у фінальній формі 9 червня 2026
https://doi.org/10.3842/kau.2026.phys.01

Анотація. У статті досліджується вплив космічного вивітрювання на поверхні астероїдів 24 сімейств різної таксономії (11 сімейств S-типу та 13 C-типу) і віку на основі фотометричних даних каталогів SDSS MOC4, Gaia та SkyMapper. Визначено вік кожного сімейства за допомогою апроксимації V-shape у просторі велика піввісь — абсолютна зоряна величина. Додатково проаналізовано спектральні характеристики астероїдів та досліджено залежність параметра a^*, який характеризує нахил спектру, від віку сімейств. Окрім цього, встановлено кореляційні залежності між параметром a^* і логарифмом віку для сімейств S-типу та C-типу. Нарешті, виявлено різний характер еволюції спектрального нахилу з віком для астероїдів різної таксономії: у сімейств C-типу параметр a^* зменшується з віком, тоді як у сімейств S-типу — зростає. Отримані результати розширюють уявлення про механізми космічного вивітрювання та їхній вплив на фізичні властивості поверхонь астероїдів.

Ключові слова: космічне вивітрювання; V-shape; показник кольору; таксономія; астероїдні сімейства; SDSS; Gaia; SkyMapper.